

# Supporting Information

## Antenna enhanced graphene THz emitter and detector

Jiayue Tong<sup>1</sup>, Martin Muthee<sup>2</sup>, Shao-Yu Chen<sup>1</sup>, Sigfrid K. Yngvesson<sup>2</sup> and Jun Yan<sup>1</sup>

<sup>1</sup>Department of Physics, University of Massachusetts, Amherst, Massachusetts 01003,

USA

<sup>2</sup>Department of Electrical and Computer Engineering, University of Massachusetts,

Amherst, Massachusetts 01003, USA

### S1. Additional THz emission spectrum

The emission characteristics of the  $45 \times 31 \mu\text{m}^2$  antenna fed by a monolayer graphene piece in the center are robust and are not sensitive to a particular sample. Figure S1 a,b show the optical microscope image and the THz spectrum of another device (D4) that we measured extensively. The THz spectrum shows a peak centered around 1.9 THz similar to results in the main text.

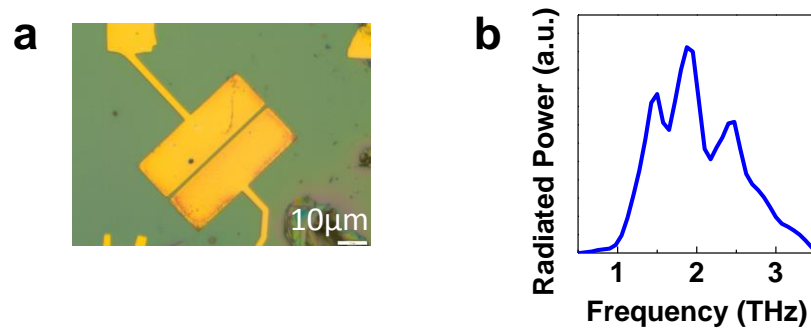


**Figure S1.** (a) Optical microscope image of device D4. (b) Measured THz radiation spectrum from D4.

## S2. Additional data of detectors with different contact designs

In addition to the half-edge-contacted device D3 with different metals for the two electrodes as described in the main text, we fabricated and measured detectors with other designs that also break the source-drain mirror symmetry. Figure S2 (a) shows the optical microscope image of a half-edge-contacted device D5 with both source and drain electrodes made by chromium/gold. This device also gives a polarization dependent response that is peaked when the THz electric field is perpendicular to the slot, as shown in Fig.S2 (b). The maximum responsivity at zero gate voltage is however, only 0.18V/W, about 6 times smaller than that of device D3. We also made several devices that are top-contacted by palladium for source and gold for drain respectively (not shown). The best responsivity that was achieved is less than 1mV/W.

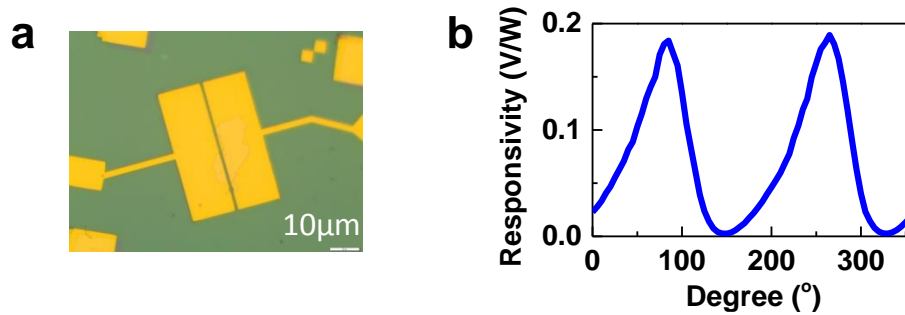


**Figure S2.** (a) Optical image of a half-edge-contacted device D5. (b) Polarization dependence of responsivity of D5 at zero gate voltage under front illumination. The peak response corresponds to the geometry in which the THz electric field is perpendicular to the slot in the antenna.

### S3. Simulation of gate voltage dependence of THz detector response

We model the thermoelectric voltage as due to the combined effects from contact metal asymmetry and contact resistance asymmetry, similar to simulations performed in [S1]. We first simulate the Fermi level as a function of position along the device channel, taking into account the different work functions of the source and drain contact metal electrodes [S2, S3]. The position-dependent conductivity is calculated according to the Fermi level, and the different contact resistances are added to the source and drain similar to [S1]. The temperature profile along the device is determined numerically by solving the 1D heat transport equation as explained in Ref. [S4]. We also assumed a THz coupling efficiency of about 1%. Given Fermi level distribution and temperature profile, we calculate the Seebeck coefficient and thermoelectric field accordingly. The thermoelectric voltage is calculated by performing a line integration of the electric field along the device. In Fig. S3 we reproduce the THz response in Fig.4e (black curve) and compare with the simulation (blue curve). The simulation captures the salient features in the gate voltage dependence and achieves reasonable agreement in magnitude, indicating that our estimation of coupling efficiency is reasonable. This further explains why the response of the device does not cross zero at the same gate voltage as the Dirac point of the device.

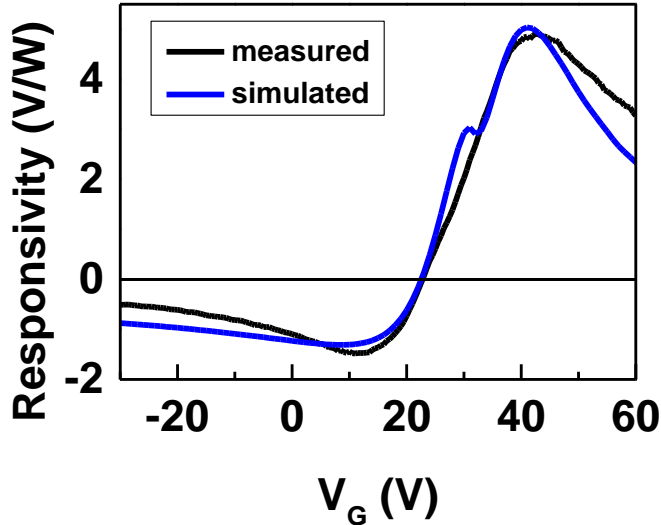


**Figure S3.** Simulated (blue) and measured (black) responsivity of D3 to 1.9THz radiation. The measured data is reproduced from Fig.4e in the main text.

## References

[S1] Cai, X.; Sushkov, A. B.; Suess, R. J.; Jadidi, M. M.; Jenkins, G. S.; Nyakiti, L. O.; Myers-Ward, R. L.; Li, S.; Yan, J.; Gaskill, D. K.; Murphy, T. E.; Drew, H. D.; Fuhrer, M. S. Sensitive room-temperature terahertz detection via the photothermoelectric effect in graphene. *Nat. Nanotechnol.* **2014**, 9, 814–819.

[S2] Khomyakov, P. A.; Starikov, A. A.; Brocks, G.; Kelly, P. J. Nonlinear screening of charges induced in graphene by metal contacts. *Phys. Rev. B* **2010**, 82, 115437.

[S3] Khomyakov, P. A.; Giovannetti, G.; Rusu, P. C.; Brocks, G.; van den Brink, J.; Kelly, P. J. First-principles study of the interaction and charge transfer between graphene and metals. *Phys. Rev. B* **2009**, 79, 195425.

[S4] Song, J. C. W.; Rudner, M. S.; Marcus, C. M.; Levitov, L. S. Hot Carrier Transport and Photocurrent Response in Graphene. *Nano Lett.* **2011**, 11, 4688-4692.